

A Nano Power CMOS Tinnitus Detector for a Fully Implantable Closed-Loop Neurodevice

Senad Hiseni¹, Chutham Sawigun¹, Sven Vanneste²⁻⁴, Eddy van der Velden⁴, Dirk De Ridder²⁻⁴ and Wouter A. Serdijn¹

¹Biomedical Electronics Group, Electronics Research Laboratory, Delft University of Technology, the Netherlands,

²Brai²n; ³Tinnitus Research Initiative; and ⁴Department of Neurosurgery, University Hospital Antwerp, Belgium
s.hiseni@tudelft.nl, w.a.serdijn@tudelft.nl

Abstract—Analog signal processing offers advantages from a power consumption viewpoint. The real-time tinnitus detection method described in this paper detects tinnitus by comparing ECoG/EEG signal energies from different locations in the brain according to a tinnitus "signature". First, the proposed strategy selects appropriate ECoG/EEG bands per channel by means of band-pass filters. Next, their extracted energies are compared to their counterparts from a different (healthy) location. Tinnitus is detected only if higher theta and gamma energies associated with lower alpha energy, in comparison to corresponding signal energies from healthy brain region, are present. To verify the detector performance, a tinnitus CMOS detector circuit has been designed to be implemented in AMIS 0.35 μ m technology (I3T25) and has been verified by means of simulations in Cadence using RF spectre. The final circuit operates from a 1V supply and consumes only 60nA. The applicability of the detector is verified by means of circuit simulations with real neural waveforms and is able to successfully detect tinnitus.

Index Terms—analog integrated circuits, tinnitus detector, biomedical signal processing, CMOS, neurostimulation, closed-loop, neurodevice, prosthetic devices, low-voltage, ultra low-power

I. INTRODUCTION

Tinnitus is a condition in which a patient perceives a sound that can take the form of ringing, buzzing, roaring or hissing in the absence of an external sound. Approximately a billion of people suffer from tinnitus worldwide, while in 2% - 3% of the population, tinnitus significantly degrades quality of life of the patients [1] and can lead to insomnia [2], anxiety [3] and depression [4].

Currently, there are no proven treatments for tinnitus [5]. However, recent research has shown that some tinnitus patients can benefit from electrical brain stimulation [6], [7], [8], [9]. In addition, it has been shown that there is a link between tinnitus perception and a change in the energy levels of several electrocortigraphy (ECoG) / electroencephalography (EEG) / magnetoencephalography (MEG) frequency bands [9], [10], [11], [12]. For example, the energies of theta (4-8Hz) and low-gamma (30-50Hz) waves increase, while the energy of alpha (8-12Hz) wave decreases during active tinnitus perception, as illustrated in Fig. 1. Moreover, [13] suggests that the intensity of the tinnitus perception correlates with the amount of the energy increased in the gamma band.

In order to deliver electrical brain stimulation therapy, implantable pulse generators (IPGs) are used. Herein, accurate detection of tinnitus location and intensity perception are of

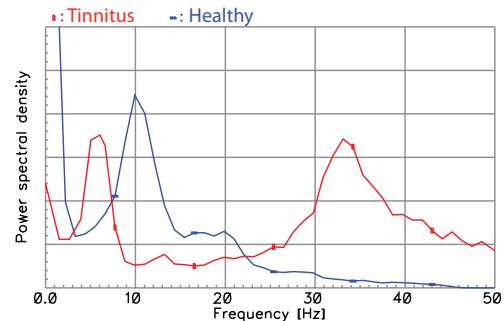


Figure 1. Illustration of typical power spectral density of signals recorded at tinnitus and healthy locations from auditory cortex in humans.

utmost importance and greatly benefit programming of the stimulation parameters at specific poles of the stimulation leads. Current programming involves, by lack of the automatic tinnitus detectors, a patient's subjective opinion by identifying changes in the intensity of the tinnitus perception in order to select an individualized stimulation therapy. This is a labor intensive, time consuming trial and error method, critically depending on the programmer's patience, the patient's concentration and is bound for failure due to the entire subjective methodology applied in the programming. Besides contributing to diagnostic and scientific research, having an automatic tinnitus detector would make it possible to automatically adapt and choose stimulation therapy, in a closed-loop (CL) manner, fully tailored to the patient's needs and the parameters selected by the physician, thereby contributing to shorter hospital stays, more effective and adaptive treatments and an improved quality of life for patients [14]. Fig. 2 illustrates such a CL neurodevice. Furthermore it could contribute to a more ecological way of stimulation as the stimulation is only activated when required.

In this paper an analog tinnitus detector enabling CL stimulation and the development of a self-regulating neurodevice capable of adjusting its parameters to the patient's needs and stimulation parameters is presented. The proposed detector relies on signals recorded from at least two electrodes placed at tinnitus and healthy locations on the auditory cortex. At first, the energies of signals in relevant ECoG/EEG bands from both locations are extracted. Secondly, their energies are compared to each other. Finally, by means of logical operators

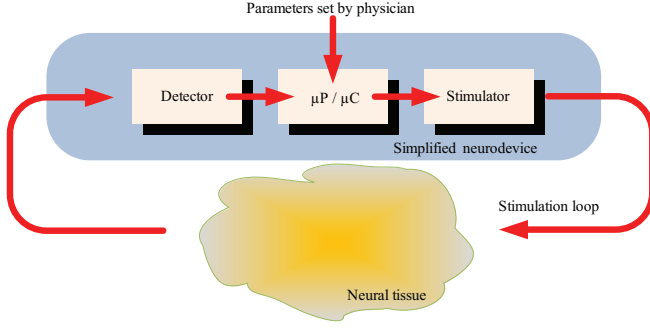


Figure 2. Closed-loop stimulation principle. Currently, in case of tinnitus, the function of detector block is performed by the patient itself.

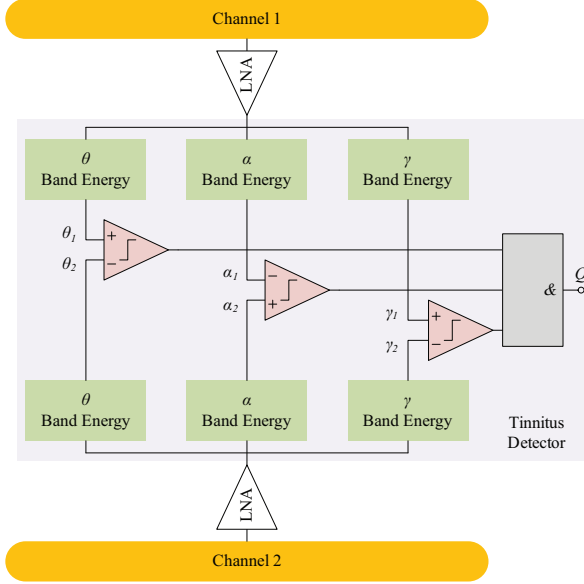


Figure 3. Block diagram of the tinnitus detection system.

the detection decision is made.

The remaining sections of the paper are organized as follows. The detector principle and system level design are reviewed in Section II. In Section III, the design of the detector circuits employing CMOS transistors operating in the subthreshold region is given. Section IV discusses the simulation results of the corresponding design. Finally, the conclusions are drawn in Section V.

II. PROPOSED TINNITUS DETECTOR

Fig. 3 shows the block diagram of the proposed tinnitus detection system. For the sake of simplicity, only one pair of channels is shown. Channel 1 and Channel 2 are representing electrodes recording from tinnitus and healthy locations at the auditory cortex, respectively, that have been found by means of fMR earlier [9]. The tinnitus detector is connected to the electrodes through low-noise amplifiers that amplify the very weak ECoG/EEG signals. There are three band energy extractors per channel, connected to an AND-gate following three comparators.

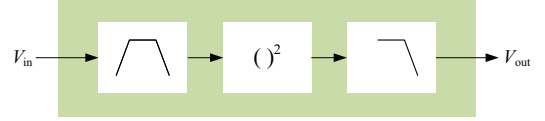


Figure 4. Energy extractor block diagram.

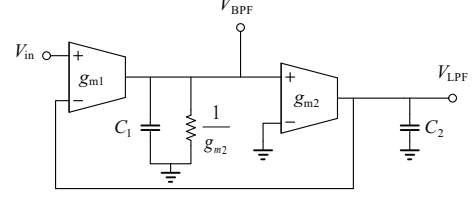


Figure 5. Band-pass and low-pass filters block diagram.

At first, the system will extract the energies of the desired frequency bands per channel. The block diagram of the energy extractor is shown in Fig. 4. It comprises a band-pass filter (BPF), a squarer and an low-pass filter (LPF). Herein, the desired ECoG/EEG band will be selected by the BPF, subsequently the signal will be squared and finally the LPF will average the signal power within the band. Next, the extracted energies of the same bands but on different channels are compared to each other. If the energies of theta and gamma waves from Channel 1 are higher than their counterparts from Channel 2, there will be a “high” input at the AND-gate. On the other hand, if the alpha wave energy from Channel 1 is lower than its counterparts from Channel 2, there will be a “high” input at the AND-gate. Tinnitus will be detected if the output of the AND-gate, defined according to

$$Q = (\theta_1 > \theta_2) \cdot (\alpha_1 < \alpha_2) \cdot (\gamma_1 > \gamma_2), \quad (1)$$

is “high”, where “.” means logical AND operation.

III. TINNITUS DETECTOR CIRCUITS

A. Energy Extractor

1) *Band-pass and low-pass filter*: Fig. 5 shows a macro-model of the biquad section employed for the band-pass and the low-pass filters which both can be realized by a single circuit, shown in Fig. 6. The values of capacitance and biasing current sources required to implement BPFs and LPFs are also shown in Fig. 6. Note that reliable bias currents as low as 6.5pA can be generated in 0.35 μ m CMOS technology [15]. The circuit contains only three transistors: transistors M_1 and M_2 are forming g_{m1} while M_3 is identical to the combination of resistor $1/g_{m2}$ and transconductor g_{m2} . The BPFs and LPFs transfer functions are defined according to

$$\frac{V_{\text{BPF}}}{V_{\text{in}}} = \frac{s \frac{g_{m1}}{C_1}}{s^2 + s \frac{g_{m2}}{C_1} + \frac{g_{m1}g_{m2}}{C_1C_2}} \quad (2)$$

and

$$\frac{V_{\text{LPF}}}{V_{\text{in}}} = \frac{\frac{g_{m1}g_{m2}}{C_1C_2}}{s^2 + s \frac{g_{m2}}{C_1} + \frac{g_{m1}g_{m2}}{C_1C_2}} \quad (3)$$

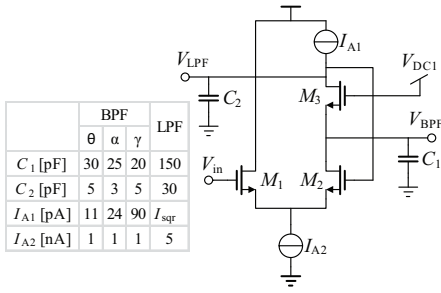


Figure 6. Band-pass and low-pass filters circuit.

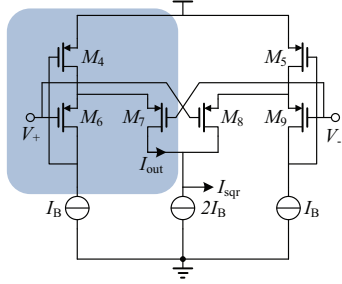


Figure 7. Hyperbolic cosine circuit.

where g_{m1} and g_{m2} are defined by $g_{m1} = (I_{A2} - I_{A1}) / [nU_T (2 + I_{A1}/I_{A2})]$ and $g_{m2} = I_{A1} / (nU_T)$, respectively. The center frequency and quality factor of the band-pass filter are found from (2) to be $\omega_n = \sqrt{(g_{m1}g_{m2}) / (C_1C_2)}$ and $Q = \sqrt{(g_{m2}C_2) / (g_{m1}C_1)}$, respectively. To realize the two second-order transfer functions shown in (2) and (3) with acceptable sizes of on-chip capacitors and very low power consumption, this circuit requires two branches of bias currents in the range of sub-nA that forces all transistors to be in their deep weak inversion.

2) *Squarer*: The shadowed area in Fig. 7 shows a circuit implementation of an exponential function. Using the exponential relationship of PMOSTs operating in weak inversion saturation [16], for $V_{SB} = 0V$ we can find that

$$I_{out} = I_B \exp\left(\frac{V_+ - V_-}{nU_T}\right) = I_B \exp\left(\frac{V_{id}}{nU_T}\right). \quad (4)$$

By connecting the exponential function circuit in anti-series at the input and parallel at the output, as shown in Fig. 7, it is

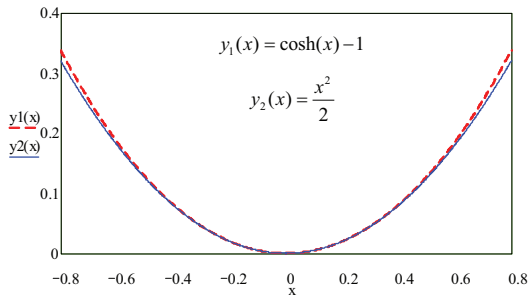


Figure 8. Hyperbolic cosine versus squaring function.

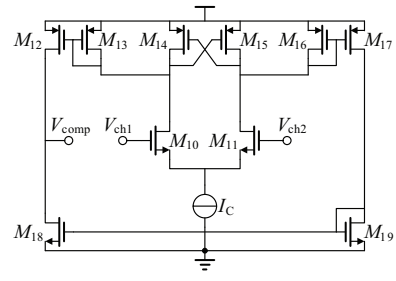


Figure 9. Voltage comparator circuit [17].

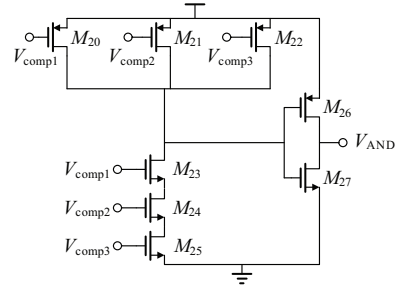


Figure 10. AND-gate circuit.

possible to create a hyperbolic cosine function circuit, ideally described by

$$\cosh(x) = \frac{e^x + e^{-x}}{2}. \quad (5)$$

Applying a Taylor series expansion to (5) we get

$$\cosh(x) = 1 + \frac{x^2}{2!} + \frac{x^4}{4!} + \frac{x^6}{6!} + \dots = \sum_{n=0}^{\infty} \frac{x^{2n}}{(2n)!}. \quad (6)$$

From (6) it can be seen that for small x values

$$\cosh(x) - 1 \approx \frac{x^2}{2}. \quad (7)$$

This similarity from (7) is illustrated in Fig. 8. For this reason, the hyperbolic cosine circuit from Fig. 7 can be used as a squarer as long as V_{id} is kept below a certain value. Moreover, by substituting (4) into (5) and subtracting bias current $2I_B$ from it, output current I_{sqr} is found to be

$$I_{sqr} = 2I_B \left[\cosh\left(\frac{V_{id}}{nU_T}\right) - 1 \right]. \quad (8)$$

B. Voltage Comparator and AND-gate

The voltage comparator circuit used is shown in Fig. 9. It is a simplified version of the comparator described in [17].

Fig. 10 depicts the circuit diagram of the AND-gate. It is constructed from a standard NAND-gate formed by $M_{20} - M_{25}$ and an inverter formed by $M_{26} - M_{27}$.

IV. SIMULATION RESULTS

The operation of the tinnitus detector circuit was verified in Cadence using RF spectre and AMIS 0.35 μ m technology (I3T25). MOS transistor widths (W) and lengths (L) were set according to Table I. The bias currents sources I_B and I_C are

Table I
TRANSISTOR DIMENSIONS

MOSFET	$M_{1-3, 13-16}$	M_{4-5}	M_{6-9}	M_{10-11}	$M_{12,17}$	M_{20-26}	$M_{18-19, 27}$
W/L [μm]	0.5/2	150/0.35	200/3.4	4/7	0.5/20	1.5/0.35	0.5/0.35

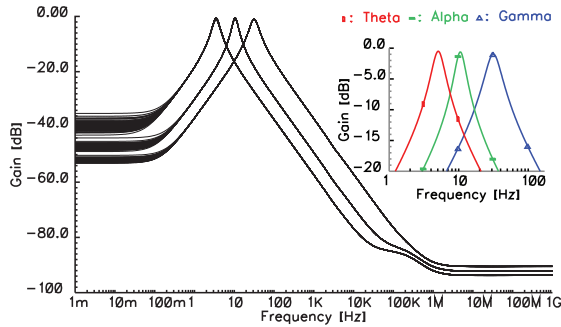


Figure 11. Monte-Carlo mismatch analysis (100 runs) of the frequency response (magnitude only) of BPFs.

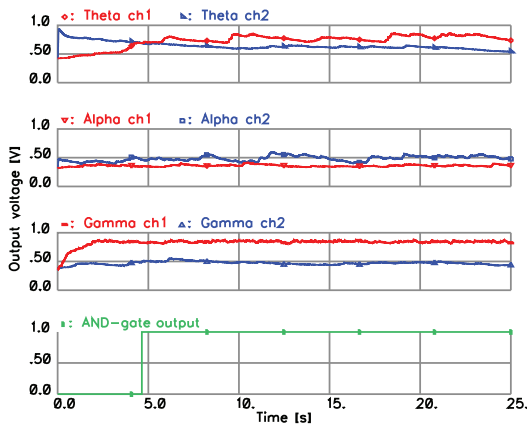


Figure 12. Transient response of the detector. Difference between gamma band signals can be used to determine severeness of tinnitus perception.

set to 1nA and 0.1nA, respectively. Supply voltage $V_{DD} = 1\text{V}$. The quiescent power consumption equals 60 nW.

Fig. 11 shows a Monte-Carlo mismatch analysis of the frequency response (magnitude only) of the BPFs. The -3dB cut-off frequencies are found at 4.1Hz and 6.5Hz for theta waves, 8.8Hz and 12.9Hz for alpha waves, and 25Hz and 42Hz for gamma waves.

Fig. 12 shows the transient response of the tinnitus circuit by using real ECoG input signal from a tinnitus patient. The voltages proportional to the energies of theta, alpha and gamma waves of both channels can be seen. As soon as (1) is satisfied, the detector output becomes high, indicative of detected tinnitus. Note that the difference between gamma energies can be used to indicate severeness of tinnitus perception.

V. CONCLUSIONS

A method to detect tinnitus by comparing the ECoG/EEG band energies from different locations in the brain has been described. The design of a CMOS tinnitus detection circuit

to be used in real-time applications has been also shown. Simulation shows that the proposed circuit consumes very little power and is able to reliably detect tinnitus. Due to the compact circuit architecture and the low power consumption, the proposed circuit is a good candidate to be used in fully implantable closed-loop neurodevices.

REFERENCES

- [1] A. Axelsson and A. Ringdahl, "Tinnitus—a study of its prevalence and characteristics.," *British Journal of Audiology*, vol. 23, no. 1, pp. 53–62, 1989.
- [2] T. Crönlein, B. Langguth, P. Geisler, and G. Hajak, "Tinnitus and insomnia," in *Tinnitus: Pathophysiology and Treatment*, vol. 166 of *Progress in Brain Research*, pp. 227–233, Elsevier, 2007.
- [3] H. Bartels, B. L. Middel, B. F. van der Laan, M. J. Staal, and F. W. Albers, "The additive effect of co-occurring anxiety and depression on health status, quality of life and coping strategies in help-seeking tinnitus sufferers," *Ear and Hearing*, vol. 29, pp. 947–956, Dec 2008.
- [4] R. A. Dobie, "Tinnitus and depression.," *Otolaryngologic Clinics of North America*, vol. 36, pp. 383–388, 2003.
- [5] R. A. Dobie, "A review of randomized clinical trials in tinnitus," *Laryngoscope*, vol. 109, pp. 1202–1211, Aug 1999.
- [6] D. De Ridder, G. De Mulder, V. Walsh, N. Muggleton, S. Sunaert, and A. Möller, "Magnetic and electrical stimulation of the auditory cortex for intractable tinnitus," *Journal of Neurosurgery*, vol. 100, no. 3, pp. 560–564, 2004.
- [7] D. De Ridder, G. De Mulder, T. Menovsky, S. Sunaert, and S. Kovacs, "Electrical stimulation of auditory and somatosensory cortices for treatment of tinnitus and pain," in *Tinnitus: Pathophysiology and Treatment*, vol. 166 of *Progress in Brain Research*, p. 377–388, Elsevier, 2007.
- [8] D. De Ridder, S. Vanneste, E. van der Loo, M. Plazier, T. Menovsky, and P. van de Heyning, "Burst stimulation of the auditory cortex: a new form of neurostimulation for noise-like tinnitus suppression," *Journal of Neurosurgery*, vol. 112, no. 6, pp. 1289–1294, 2010.
- [9] D. De Ridder, E. van der Loo, S. Vanneste, S. Gais, M. Plazier, S. Kovacs, S. Sunaert, T. Menovsky, and P. van de Heyning, "Theta-gamma dysrhythmia and auditory phantom perception," *Journal of Neurosurgery*, vol. 114, no. 4, pp. 912–921, 2011.
- [10] N. Weisz, S. Müller, W. Schlee, K. Dohrmann, T. Hartmann, and T. Elbert, "The neural code of auditory phantom perception," *The Journal of Neuroscience*, vol. 27, no. 6, pp. 1479–1484, 2007.
- [11] R. R. Llinás, U. Ribary, D. Jeanmonod, E. Kronberg, and P. P. Mitra, "Thalamocortical dysrhythmia: A neurological and neuropsychiatric syndrome characterized by magnetoencephalography," *Proceedings of the National Academy of Sciences*, vol. 96, no. 26, pp. 15222–15227, 1999.
- [12] W. Mühlhnickel, T. Elbert, E. Taub, and H. Flor, "Reorganization of auditory cortex in tinnitus," *Proceedings of the National Academy of Sciences of the USA*, vol. 95, no. 17, pp. 10340–10343, 1998.
- [13] E. van der Loo, S. Gais, M. Congedo, S. Vanneste, M. Plazier, T. Menovsky, P. Van de Heyning, and D. De Ridder, "Tinnitus intensity dependent gamma oscillations of the contralateral auditory cortex," *PLoS ONE*, vol. 4, p. e7396, Oct 2009.
- [14] J. Lee, H.-G. Rhew, D. R. Kipke, and M. P. Flynn, "A 64 channel programmable closed-loop neurostimulator with 8 channel neural amplifier and logarithmic ADC," *Solid-State Circuits, IEEE Journal of*, vol. 45, pp. 1935–1945, sept. 2010.
- [15] A. J. Casson and E. Rodriguez-Villegas, "A 60 pW g_m/C continuous wavelet transform circuit for portable EEG systems," *Solid-State Circuits, IEEE Journal of*, vol. 46, pp. 1406–1415, june 2011.
- [16] E. Vittoz and J. Fellrath, "CMOS analog integrated circuits based on weak inversion operations," *Solid-State Circuits, IEEE Journal of*, vol. 12, pp. 224–231, jun 1977.
- [17] D. J. Allstot, "A precision variable-supply CMOS comparator," *Solid-State Circuits, IEEE Journal of*, vol. 17, pp. 1080–1087, dec 1982.